Flutter Suppression of Cantilevered Plate Wing using Piezoelectric Materials

Kanjuro Makihara*, Junjiro Onoda and Kenji Minesugi*****

Institute of Space and Astronautical Science(ISAS)
Japan Aerospace Exploration Agency(JAXA)
3-1-1 Yoshinodai, Sagamihara, Kanagawa, 229-8510, Japan

Abstract

The supersonic flutter suppression of a cantilevered plate wing is studied with the finite element method and the quasi-steady aerodynamic theory. We suppress wing flutter by using piezoelectric materials and electric devices. Two approaches to flutter suppression using piezoelectric materials are presented; an energy-recycling semi-active approach and a negative capacitance approach. To assess their flutter suppression performances, we simulate flutter dynamics of the plate wing to which piezoelectric patches are attached. The critical dynamic pressure drastically increases with our flutter control using a negative capacitor.

Key Word: Flutter, Piezoelectric, Energy-Recycling, Semi-Active, Negative Capacitance

Nomenclature

a_∞	: speed of sound in air
c	: Young's modulus
D_z, E_z	: z-directional electric displacement and electric field
$\boldsymbol{f}$	: external disturbance vector
$\boldsymbol{F}$	: feedback matrix
h_{xz}	: piezoelectric coefficient
n_p	: number of piezoelectric patches
$\boldsymbol{N}_\mathrm{F}$	: shape function of FEM element
p	: pressure acting on the plate
p_∞	: air pressure
$\boldsymbol{Q}$	: electric charge vector of piezoelectric patches
$u(x,y,t)$	: z-directional displacement of wing
U	: flight speed
$\boldsymbol{V}$	: voltage vector of piezoelectric patches
$\boldsymbol{W}_1, \boldsymbol{W}_2$	: weighting matrices in Eq. (29)
$\boldsymbol{x}$	: assembled displacement vector at FEM nodes
β_{zz}^S	: z-directional dielectric coefficient at constant strain
$\boldsymbol{\epsilon}$, $\boldsymbol{\sigma}$	: strain and stress vectors

* Aerospace Project Research Associate
E-mail : kanjuro@svs.eng.isas.jaxa.jp
** Professor
*** Associate Professor

ρ, ν : density and Poisson's ratio
ρ_∞ : air density
ξ : modal displacement vector

superscript
D : constant electric displacement
S : constant strain
T : transpose

subscript
p : piezoelectric patch
pj : jth piezoelectric patch
w : wing structure without piezoelectric patches

Introduction

Flutter is a self-excited aeroelastic phenomenon, and is caused by the interactions between wings' structural motions and aerodynamics loads exerted on the wing. The wing flutter occurs most frequently in high-speed, i.e., transonic, supersonic, and hypersonic flow [1, 2]. Lin et al. [3] studied flutter characteristics by using triangular finite elements and the doublet-lattice method. Lottati [4] investigated the structural and aerodynamic damping effect on the flutter speed with a composite plate wing. A variety of studies for flutter dynamics have been done, such as flutter prediction [5], flutter dynamics caused by thermal loads [6], optimal design for avoiding flutter using lamination parameters [7], and robust structural optimization of wings [8].

The use of advanced smart materials in aerospace engineering can lead to the development of new design concept. Smart materials include piezoelectric materials, shape memory alloys, magnetorestrictive materials, and so forth. The new design concept is to change structural dynamics by generating force or deformation. Various active flutter suppression methods [9–12] have been studied. Zhou et al. [9] and Moon and Hwang [10] used the linear quadratic regulator (LQR) theory to suppress nonlinear panel flutter. Han et al. [11] designed a μ-synthesis controller to enhance flutter suppression performance despite parametric uncertainties. Raja et al. [12] exploited multilayered piezoelectric actuators and sensors for constructing a linear quadratic gaussian (LQG) controller to suppress the flutter of a composite plate. In contrast, in the light of passive vibration suppression, shunting piezoelectric devices that are composed of an inductor and a resistor was proposed by Hagood and von Flotow [13] and Wu. [14] Such an inductive circuit has an electrical resonance that can work as dynamic mass dampers do. Moon and Kim [15] and Agneni [15] applied this passive method to flutter suppression and they demonstrated satisfactory suppression performances. However, the flutter suppression performance of this passive method is degraded when the frequency of the electrical resonance is slightly different from the frequency of the structure. That is why the passive method possesses limited robustness against model errors, and is not suitable for the systems whose structural frequencies can shift due to aerodynamic influence.

Meanwhile, semi-active controls using piezoelectric materials were recently proposed. Clark [17] proposed a switch-shunting damper (SSD) implemented with a switchable stiffness element composed of a piezoelectric material. Richard et al. [18] proposed an energy-dissipative method

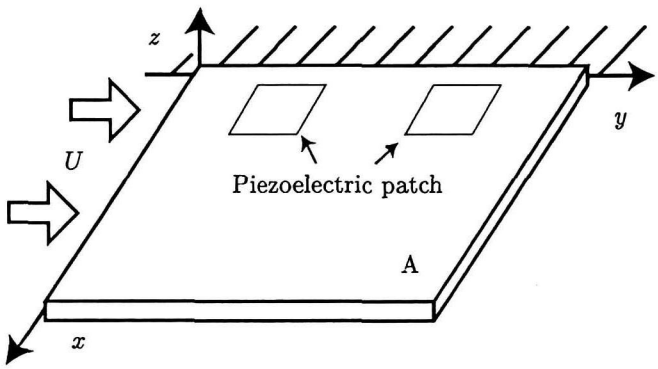

Fig. 1. Plate wing with piezoelectric patches

whereby a switch in a shunt circuit is controlled in synchronization with the structural vibration. This method makes good use of the passive energy-dissipation mechanism of an electrical resistor. In particular, Onoda et al. [19] proposed another semi-active vibration suppression method using an inductive circuit composed of an inductor, a selector switch, and two diodes. By controlling the selector switch, the mechanical energy is converted to electrical energy, and the converted electrical energy is recycled to efficiently suppress vibration rather than immediately being dissipated. This energy-recycling semi-active approach has previously been analyzed from the viewpoint of energy flow [20] and used in various engineering applications, [21–25] for example, a self-sensing system, [22] an energy-harvesting device, [23,24] and a disturbance isolator. [25] This energy-recycling mechanism is quite an excellent feature for achieving powerful vibration suppression. Therefore, we expect that this energy-recycling semi-active approach can attenuate wing flutter, which is a forceful vibration.

In this study, wing flutter is suppressed by using a smart circuit composed of piezoelectric materials and electric devices. Two approaches of flutter suppression are presented and assessed in the supersonic flutter problem.

Governing equations for piezoelectric system

A cantilevered plate wing (Fig. 1) is considered to investigate flutter suppression. Our plate wing simulates wings of sounding rockets flying at a supersonic speed. Thus, we assume that the plate is subject to supersonic flutter. Piezoelectric patches are attached to the wing to generate bending moment for flutter suppression. In practice, patches attached on the wing surface may have negative effects on fluid dynamics, because they cause the discontinuity of the wing surface. Furthermore, the patches may adversely be affected by the heat caused by aerodynamic interference. However, in this paper, we do not consider these issues, but we need to develop implanted piezoelectric actuators, such as piezoelectric fibers embedded in composite plates.

Aerodynamic pressure

Aerodynamics pressure under high supersonic, i.e., $\sqrt{2} < M$, is described by a quasi-steady first-order piston theory. [26] The pressure acting on the plate flying at a speed of U is given

by

$$p - p_\infty = \frac{2q}{\sqrt{M^2-1}}\left[\frac{\partial u}{\partial y} + \frac{M^2-2}{M^2-1}\frac{1}{U}\frac{\partial u}{\partial t}\right] \tag{1}$$

where

$$q \equiv \frac{1}{2}\rho_\infty U^2, \quad M \equiv \frac{U}{a_\infty} \tag{2}$$

Considering pressure on the both sides, we can express the resultant pressure exerting on the wing, $p_a(x,y,t)$, as

$$p_a(x,y,t) \equiv \frac{-4q}{\sqrt{M^2-1}}\left[\frac{\partial u}{\partial y} + \frac{M^2-2}{M^2-1}\frac{1}{U}\frac{\partial u}{\partial t}\right] \tag{3}$$

Equations for Wing and Piezoelectric Patches

Piezoelectric patches shown in Fig. 1 are assumed to be polarized in the thickness direction (z direction) and to be isotropic in the in-plane direction (x-y plane). Hence, their constitutive equations [27] are given by

$$\boldsymbol{\sigma}_p = \tilde{\boldsymbol{c}}_p^D \boldsymbol{\epsilon}_p - \boldsymbol{h} D_z, \quad E_z = -\boldsymbol{h}^{\mathrm{T}} \boldsymbol{\epsilon}_p + \beta_{zz}^S D_z \tag{4}$$

where

$$\boldsymbol{\sigma}_p \equiv \begin{Bmatrix} \sigma_x \\ \sigma_y \\ \tau_{xy} \end{Bmatrix}, \quad \boldsymbol{\epsilon}_p \equiv \begin{Bmatrix} \epsilon_x \\ \epsilon_y \\ \gamma_{xy} \end{Bmatrix}, \quad \boldsymbol{h} \equiv \begin{Bmatrix} h_{xz} \\ h_{xz} \\ 0 \end{Bmatrix}, \quad \tilde{\boldsymbol{c}}_p^D \equiv \frac{c_p^D}{1-\nu_p^2}\begin{bmatrix} 1 & \nu_p & 0 \\ \nu_p & 1 & 0 \\ 0 & 0 & \frac{1-\nu_p}{2} \end{bmatrix} \tag{5}$$

The stress-strain relation of a wing is written as

$$\boldsymbol{\sigma}_w = \tilde{\boldsymbol{c}}_w \boldsymbol{\epsilon}_w \tag{6}$$

where

$$\tilde{\boldsymbol{c}}_w \equiv \frac{c_w}{1-\nu_w^2}\begin{bmatrix} 1 & \nu_w & 0 \\ \nu_w & 1 & 0 \\ 0 & 0 & \frac{1-\nu_w}{2} \end{bmatrix} \tag{7}$$

The linear strain-displacement relation based on the Kirchhoff-Love assumption is

$$\boldsymbol{\epsilon} = -z\left[\frac{\partial^2}{\partial x^2}, \frac{\partial^2}{\partial y^2}, 2\frac{\partial^2}{\partial x \partial y}\right]^{\mathrm{T}} u(x,y,t) \tag{8}$$

On the surface of our wing, n_{p} pieces of piezoelectric patches are attached, and the jth patch is attached at position $x_{1j} \le x \le x_{2j}$, $y_{1j} \le y \le y_{2j}$ and $z_{1j} \le z \le z_{2j}$. To ensure the generality of the theoretical analysis, a multiple-input-multiple-output (MIMO) system is considered. Using Hamilton's principle, we can construct

$$\int_{t_1}^{t_2}\left[\delta T_w - \delta U_w + \sum_{j=1}^{n_{\mathrm{p}}}(\delta T_{pj} - \delta U_{pj}) + \delta W\right] \mathrm{d}t = 0 \tag{9}$$

The kinetic energy of the wing, T_w, is

$$T_w \equiv \int_V \frac{1}{2}\rho_w \left(\frac{\partial u}{\partial t}\right)^2 \mathrm{d}V \tag{10}$$

The strain energy of the wing, U_w, is given by

$$U_w \equiv \frac{1}{2}\int_V \boldsymbol{\sigma}_w^{\mathrm{T}}\boldsymbol{\epsilon}_w \, \mathrm{d}V \tag{11}$$

The kinetic energy of the jth piezoelectric patch, T_{pj}, has the form,

$$T_{pj} \equiv \int_{V_{pj}} \frac{1}{2}\rho_{pj}\left(\frac{\partial u}{\partial t}\right)^2 g_j(x,y,z)\mathrm{d}V \tag{12}$$

where $g_j(x,y,z)$ is defined with Heaviside functions as

$$g_j(x,y,z) \equiv [H(x-x_{1j}) - H(x-x_{2j})]$$
$$\times [H(y-y_{1j}) - H(y-y_{2j})] \times [H(z-z_{1j}) - H(z-z_{2j})] \tag{13}$$

The mechanical and electrical energy of the jth piezoelectric patch, U_{pj}, is

$$U_{pj} \equiv \frac{1}{2}\int_{V_{pj}} (\boldsymbol{\sigma}_p^{\mathrm{T}}\boldsymbol{\epsilon}_p + E_z D_z)\mathrm{d}V \tag{14}$$

Virtual work, δW, can be written as

$$\delta W \equiv \int_S \delta u[f(x,y,t) + p_a(x,y,t)]\mathrm{d}S + \sum_{j=1}^{n_p} V_j \int_{S_{pj}} \delta D_{zj} g_j(x,y,z)\mathrm{d}S \tag{15}$$

where $f(x,y,t)$ is external force normal to the wing, and V_j is voltage applied to the jth piezoelectric patch as a generalized external force.

Controller Based on Finite Element Formulation

The ACM FEM element, [28] a four-node non-conforming plate element, is employed to discretize partial derivative equations of motion. From Eqs. (3)-(15), the equation of motion for the cantilevered wing with multiple piezoelectric patches can be expressed as

$$\boldsymbol{M}\ddot{\boldsymbol{x}} + \boldsymbol{K}\boldsymbol{x} = \boldsymbol{B}_p\boldsymbol{Q} - \chi\boldsymbol{A}\boldsymbol{x} + \boldsymbol{f} \tag{16}$$

and

$$\boldsymbol{V} = -\boldsymbol{B}_p^{\mathrm{T}}\boldsymbol{x} + \boldsymbol{C}_p^{-1}\boldsymbol{Q} \tag{17}$$

where

$$\boldsymbol{M} \equiv \sum_{\mathrm{ele}} \int_{V+V_p} \rho \boldsymbol{N}_{\mathrm{F}}^{\mathrm{T}}\boldsymbol{N}_{\mathrm{F}} \, \mathrm{d}V \tag{18}$$

$$\boldsymbol{K} \equiv \sum_{\mathrm{ele}} \int_{V+V_p} z^2 \boldsymbol{B}_{\mathrm{F}}^{\mathrm{T}}\tilde{\boldsymbol{c}}\boldsymbol{B}_{\mathrm{F}} \, \mathrm{d}V \tag{19}$$

$$\boldsymbol{A} \equiv \sum_{\mathrm{ele}} \int_S \boldsymbol{N}_{\mathrm{F}}^{\mathrm{T}} \frac{\partial \boldsymbol{N}_{\mathrm{F}}}{\partial y} \, \mathrm{d}S \tag{20}$$

$$\boldsymbol{B}_p \equiv \sum_{\mathrm{ele}} \int_{V_p} \left(\frac{z}{S_{\mathrm{ele}}}\right) \boldsymbol{B}_{\mathrm{F}}^{\mathrm{T}}\boldsymbol{h} \, \mathrm{d}V \tag{21}$$

$$\boldsymbol{B}_{\mathrm{F}} \equiv \left[\frac{\partial^2 \boldsymbol{N}_{\mathrm{F}}}{\partial x^2}, \frac{\partial^2 \boldsymbol{N}_{\mathrm{F}}}{\partial y^2}, 2\frac{\partial^2 \boldsymbol{N}_{\mathrm{F}}}{\partial x \partial y}\right]^{\mathrm{T}} \tag{22}$$

$$\chi \equiv \frac{4q}{\sqrt{M^2-1}} \tag{23}$$

Here, S_{ele} is the area of each element and V_p is the volume corresponding to piezoelectric patches. The damping term, i.e., the second term in Eq. (3), is neglected for simplicity. We use transformation, $\boldsymbol{x} = \boldsymbol{\Phi}\boldsymbol{\xi}$, and introduce a modal damping ratio of ζ to all vibration modes, so Eq. (16) becomes

$$\ddot{\boldsymbol{\xi}} + \boldsymbol{\Xi}\dot{\boldsymbol{\xi}} + (\boldsymbol{\Omega} + \chi\boldsymbol{\Phi}^{\mathrm{T}}\boldsymbol{A}\boldsymbol{\Phi})\boldsymbol{\xi} = \boldsymbol{\Phi}^{\mathrm{T}}\boldsymbol{B}_p\boldsymbol{Q} + \boldsymbol{\Phi}^{\mathrm{T}}\boldsymbol{f} \tag{24}$$

where

$$\boldsymbol{\Phi} \equiv [\phi_1, \phi_2, \ldots, \phi_n],\ \boldsymbol{\Omega} \equiv \mathrm{diagonal}[\omega_k^2],\ \boldsymbol{\Xi} \equiv \mathrm{diagonal}[2\zeta\omega_k] \tag{25}$$

ω_k and ϕ_k are obtained by solving the eigenvalue problem for the homogenous part of Eq. (16) when the aerodynamics is neglected (i.e., $\chi = 0$). The modal equation (24) can be rewritten as

$$\dot{\boldsymbol{z}} = \boldsymbol{A}\,\boldsymbol{z} + \boldsymbol{B}\,\boldsymbol{Q} + \boldsymbol{G}\,\boldsymbol{f} \tag{26}$$

where

$$\boldsymbol{z} \equiv [\boldsymbol{\xi}^{\mathrm{T}}, \dot{\boldsymbol{\xi}}^{\mathrm{T}}]^{\mathrm{T}},\ \boldsymbol{A} \equiv \begin{bmatrix} \boldsymbol{0} & \boldsymbol{I} \\ -\boldsymbol{\Omega} - \chi\boldsymbol{\Phi}^{\mathrm{T}}\boldsymbol{A}\boldsymbol{\Phi} & -\boldsymbol{\Xi} \end{bmatrix} \tag{27}$$

$$\boldsymbol{B} \equiv \begin{bmatrix} \boldsymbol{0} \\ \boldsymbol{\Phi}^{\mathrm{T}}\boldsymbol{B}_p \end{bmatrix},\ \boldsymbol{G} \equiv \begin{bmatrix} \boldsymbol{0} \\ \boldsymbol{\Phi}^{\mathrm{T}} \end{bmatrix} \tag{28}$$

If $\boldsymbol{Q}$ in Eq. (26) can be regarded as an active control input, the LQR theory specifies that the control input, $\boldsymbol{Q}$, that minimizes the performance index

$$J \equiv \int_0^\infty (\boldsymbol{z}^{\mathrm{T}}\boldsymbol{W}_1\boldsymbol{z} + \boldsymbol{Q}^{\mathrm{T}}\boldsymbol{W}_2\boldsymbol{Q})\,\mathrm{d}t \tag{29}$$

is

$$\boldsymbol{Q} = \boldsymbol{Q}_T \equiv -\boldsymbol{F}\boldsymbol{z} \tag{30}$$

In the standard guideline of the LQR active control, the first and second terms on the right-hand side in Eq. (29) correspond to the state energy and the control input energy, respectively, with appropriate $\boldsymbol{W}_1$ and $\boldsymbol{W}_2$. The performance index, J, comprises the two competing factors. However, our semi-active method does not provide any control energy based on $\boldsymbol{Q}_T$, but it only makes reference to the polarity of $\boldsymbol{Q}_T$ for its switching operation, as will be discussed. The meaning of $\boldsymbol{W}_1$ and $\boldsymbol{W}_2$ in switching control systems is different from the standard guideline, according to Ref. [20]

Flutter suppression methods

Approach 1: Piezoelectric switching control

In general, active vibration controls supply electrical energy (voltage or charge) into piezoelectric materials to generate actuation force. In contrast to such an active control, we intend to implement a semi-active control by using a piezoelectric material and a switch. That is, only by controlling the switch of the circuit connected to a piezoelectric material, do we suppress vibration. One simple semi-active method using a piezoelectric material is to suppress vibration by alternately opening and closing the switch connected to the material. This method is referred to as state-switching damper (SSD) method, [17] and it makes use of the stiffness shift of a piezoelectric material. The SSD has the following control logic; when the mass is moving towards the equilibrium point, the piezoelectric material is short-circuited, and when the mass

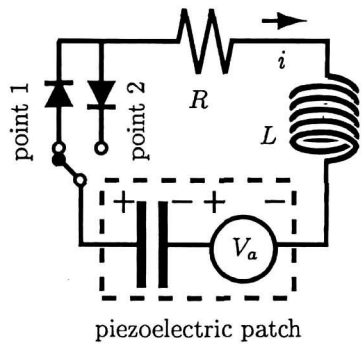

Fig. 2. Circuit for energy-recycling semi-active approach

is moving away from the equilibrium point, the material is open-circuited. To the best of our knowledge, this control can be employed only for single-degree-of-freedom (SDOF) systems.

In contrast, we will adopt another semi-active approach; the piezoelectric material is short-circuited for a brief time in synchronization with vibration, and it is open-circuited the rest of the time. Our semi-active approach is referred to as energy-recycling semi-active method because it inherently possesses an energy-recycling mechanism, as will be described. The basic notion of the energy-recycling semi-active method was comprehensively described in Refs. [19,20] but a brief explanation of the method is presented here for a better understanding of what follows.

The energy-recycling semi-active method uses an electric circuit connected to the piezoelectric material. The circuit is composed of a selector switch, an inductor, a resistor, and two diodes, as shown in Fig. 2. The piezoelectric material is modeled as a capacitor and a voltage generator, V_a, that is caused by the piezoelectric effect. As Eq. (30) indicates, the control input, Q_T, can be obtained from active control schemes. According to Ref. [19] one switching strategy of suppressing semi-actively vibration involves controlling the jth switch so that Q_j has the same polarity as Q_{Tj} and the absolute value of Q_j is as large as possible. One switching logic is

$$\begin{aligned} &\textit{when } Q_{Tj} < 0, && j\textit{th switch to point 1} \\ &\textit{when } Q_{Tj} > 0, && j\textit{th switch to point 2} \end{aligned} \tag{31}$$

Since our semi-active method simply changes switch connection, it never increases vibration energy by its switching action. In this regard, our semi-active approach is safer than the active controls that usually have the danger of instability, such as spillover. Furthermore, making reference to the modern active control input enables our semi-active method to be applicable to MIMO systems. This advanced semi-active method can selectively suppress multiple-mode vibrations, and can control multiple piezoelectric actuators cooperatively (in the sense of the centralized-control) rather than independently.

As will be seen later, in flutter problems, modal frequencies can shift depending on the dynamic pressure. In such a case, modal detection or estimation is impractical for actual systems. Then, it is reasonable that Q_T should be modified to a more general one without modal information. One way to implement switching controls without modal information is adopting semi-active flutter suppression based on the direct velocity feedback method, describing Q_{Tj} in Eq. (31) as

$$Q_{Tj} \equiv -\dot{\epsilon}_{pj} \tag{32}$$

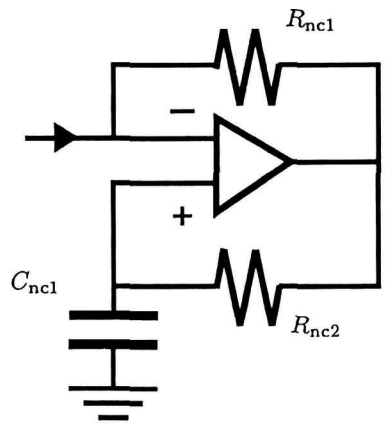

Fig. 3. Negative capacitor using an operational amplifier

where ϵ_{pj} is the strain at the position of the jth piezoelectric patch.

Various types of sensors, such as strain gauges or acceleration meters, can be employed to detect strain. As well known, additional piezoelectric patches can be used as strain sensors. In contrast, an innovative self-sensing method proposed by Makihara et al. [22] enables a single piezoelectric patch to function as an actuator and a sensor at the same time, instead of installing sensors or using sensitive bridge-circuits. However, the attractive self-sensing technique was not used for this study to focus only on flutter suppression assessment.

Approach 2: Negative capacitance control

Recently, some researchers proposed vibration control methods using piezoelectric materials and negative capacitors. [29–31] A negative capacitor possesses quite a different electrical mechanism from positive capacitors. As shown in Fig. 3, a negative capacitor can be emulated with an operational amplifier, resistors (R_{nc1}, R_{nc2}), and a capacitor (C_{nc1}). By using this emulating circuit, we obtain the negative value of capacitance as

$$C^{\mathrm{nc}} \equiv -C_{\mathrm{nc1}} \frac{R_{\mathrm{nc1}}}{R_{\mathrm{nc2}}} \tag{33}$$

where $C_{\mathrm{nc1}}, R_{\mathrm{nc1}}, R_{\mathrm{nc2}}$ are positive. When a negative capacitor is connected to a piezoelectric patch, the Kirchhoff equation for the jth circuit becomes

$$Q_j = -\frac{\gamma_j^{\mathrm{nc}}}{1-\gamma_j^{\mathrm{nc}}} [\boldsymbol{C}_p \boldsymbol{B}_p^{\mathrm{T}} \boldsymbol{x}]_j \tag{34}$$

where

$$\gamma_j^{\mathrm{nc}} \equiv -\frac{C_j^{\mathrm{nc}}}{[\boldsymbol{C}_p]_j} \tag{35}$$

Here, Q_j is the charge stored in the jth piezoelectric patch and $[\,]_j$ denotes a value corresponding to the jth circuit. By combining Eq. (16) and Eq. (34), we derive a new stiffness matrix, $(\boldsymbol{K} + \boldsymbol{B}_p \boldsymbol{\Gamma} \boldsymbol{C}_p \boldsymbol{B}_p^{\mathrm{T}})$, where

$$\boldsymbol{\Gamma} \equiv \mathrm{diagonal}[\frac{\gamma_j^{\mathrm{nc}}}{1-\gamma_j^{\mathrm{nc}}}] \tag{36}$$

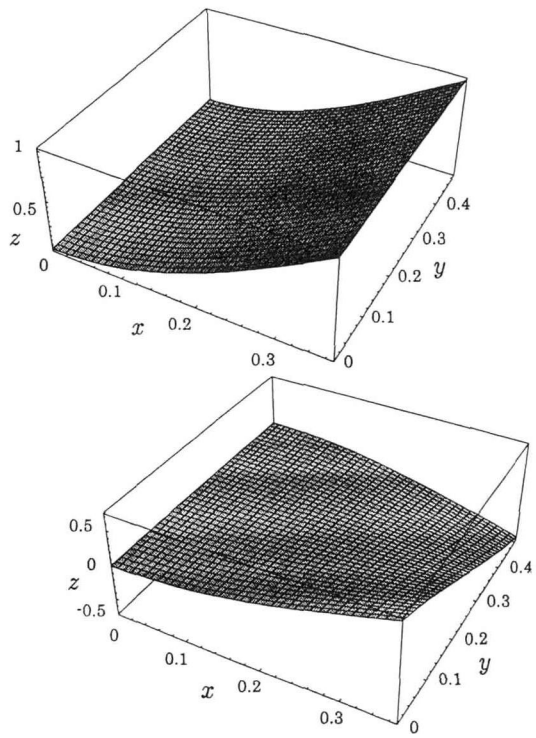

Fig. 4. Mode shapes of cantilevered plate wing (top: first mode, bottom: second mode).

When we determine γ_j^{nc} to be $0 < \gamma_j^{nc} < 1$, the additional stiffness matrix is a positive-definitive matrix, which increases the wing's stiffness.

Numerical simulation

We conducted numerical simulation for flutter suppression on the plate wing (Fig. 1). The wing had an area of 0.37 by 0.49 m and a thickness of 6.75 mm, and was made of Titanium alloy (Ti-6Al-4V). It was rigidly supported on its one boundary, i.e., $x = 0$. A piezoelectric material ($P_b(Z_r \cdot T_i)O_3$ ceramic type, 154 × 175 × 5 mm) was attached at $0 \leq x \leq 0.154$ and $0.28 \leq y \leq 0.455$ on the wing. The first and the second mode frequencies for an open circuit (i.e., constant charge) were 43.0 Hz and 84.5 Hz, respectively, for the plate attached to the piezoelectric patch while the aerodynamic influence was neglected. Fig. 4 shows two mode shapes of the cantilevered plate wing. Other simulation parameters are listed on Table 1. These simulation parameters were based on actual materials.

Eigenvalue analysis

Equation (16) is reduced into eigenvalue problem;

$$\det[-\lambda \boldsymbol{M} + \boldsymbol{K} + \chi \boldsymbol{A}] = 0 \tag{37}$$

Table 1. Parameter values of piezoelectric patch and wing

	Piezo	Wing	unit
Young's modulus	6.40×10^{10}	1.13×10^{11}	N/m^2
density	8.10×10^3	4.47×10^3	kg/m^3
poisson's ratio	0.32	0.31	–
dielectric coefficient (β_{zz}^S)	1.95×10^7	–	Vm/C
piezoelectric coefficient (h_{zz})	4.67×10^8	–	V/m

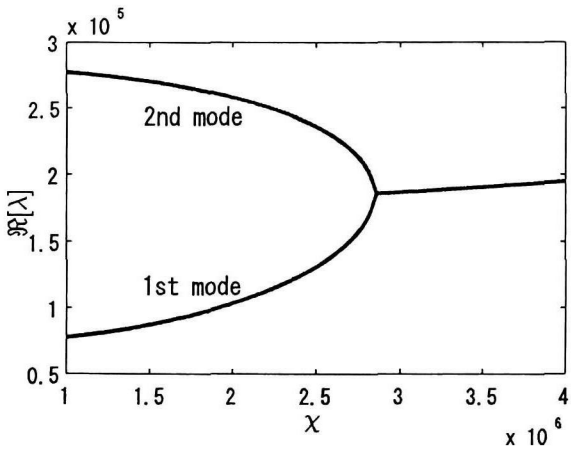

Fig. 5. Real part of eigenvalues as a function of dynamic pressure (no control)

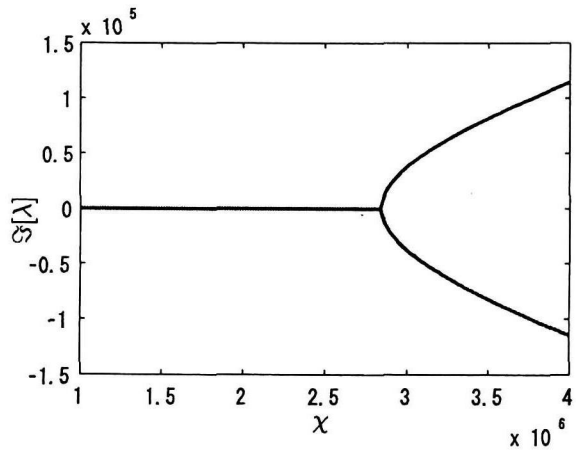

Fig. 6. Imaginary part of eigenvalues as a function of dynamic pressure (no control)

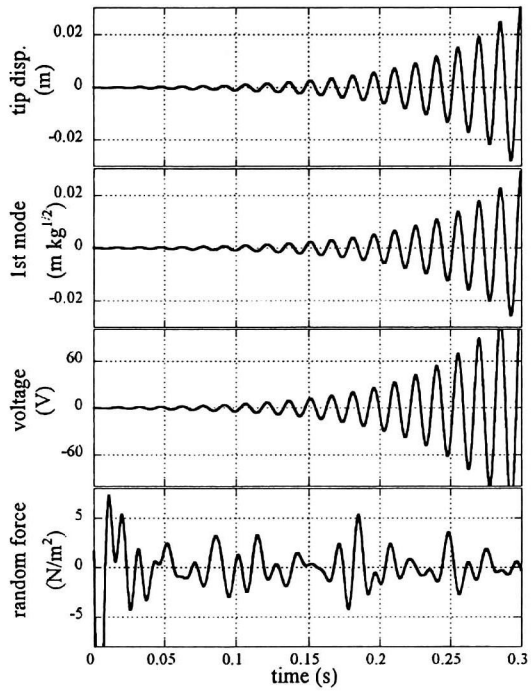

Fig. 7. History of the wing at a critical dynamic pressure (no control)

where λ is a complex eigenvalue. Since the eigen-analysis is conducted for a no-control system, the control input ($\vec{Q}$) and the external disturbance ($\vec{f}$) are neglected. Fig. 5 plots the real part of eigenvalues as a function of dynamic pressure parameter, χ. Two values become close to each other as χ increases. When $\chi = 2.86 \times 10^6$, the two become one, i.e., $\Re[\lambda] = 1.86 \times 10^3$. With this critical value of χ, the wing experiences flutter phenomenon. This figure shows loci of only the first and the second modes. Since this critical point indicates smallest dynamic pressure among all critical values, we focus only on the relation between two vibration modes. Fig. 6 plots imaginary part of eigenvalues as a function of χ. When χ is larger than its critical value, the imaginary parts have values other than 0.

Case study: approach 1

We simulated flutter dynamics when white-noise random force was exerted on the wing surface. The power spectral density (PSD) per unit frequency of the random force had a constant value of $0.1\,\mathrm{N}^2/\mathrm{Hz}$ in the range of 30 to 100 Hz, and its value was 0 in the rest of the frequency range. Therefore, the frequency range of nonzero PSD covered the first and the second modes.

As described in Refs. [19,20] the energy-recycling semi-active method has previously demonstrated its significant performance for general vibration suppression. It is quite reasonable that the method can suppress vibrations due to aerodynamic pressure while χ is much smaller than its critical value. Therefore, we only present the history of wing dynamics at a critical dynamic pressure, i.e., $\chi = 2.86 \times 10^6$ in Figs. 5 and 6. For comparison, Fig. 7 shows the history of wing

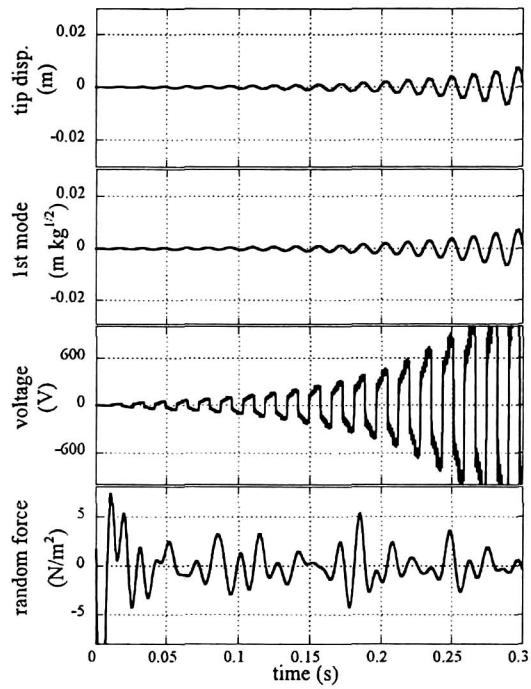

Fig. 8. History of the wing at a critical dynamic pressure (control approach 1)

dynamics without any control. At $t = 0.3$ s, tip displacement (point A in Fig. 1) reached 0.03 m. The wing suffered from strong flutter phenomenon. At this time, piezoelectric voltage was 100 V due to the piezoelectric effect. Fig. 7 shows the history of wing dynamics with control approach 1. The polarity of piezoelectric voltage was reversed every time the selector switch changed its connection point, following the control logic in Eqs. (31) and (32). Around peaks of sensor strain, ϵ_p, (i.e., peaks of tip displacement in Fig. 8), switch connection was changed, and the voltage polarity was reversed. At $t = 0.3$ s, tip displacement was only 0.008 m, but piezoelectric voltage reached as much as 1000 V because of the energy-recycling mechanism. As mentioned earlier, higher value of piezoelectric voltage or charge results in higher control performance where electric charge is regarded as a control input in Eq. (16). Comparing Figs. 7 and 8, control approach 1 did not suppress the flutter phenomenon completely in this configuration, but it worked for flutter suppression to some extent. To introduce delay into flutter growth may be a meaningful resort as practical solution for flutter problems.

Case study: approach 2

To evaluate the effectiveness of control approach 2, we conducted an eigenvalue analysis on the wing having a piezoelectric patch. For the wing with control approach 2, Eq. (16) is transformed into

$$\det[-\lambda \boldsymbol{M} + \boldsymbol{K} + \boldsymbol{B}_p \boldsymbol{\Gamma} \boldsymbol{C}_p \boldsymbol{B}_p^{\mathrm{T}} + \chi \boldsymbol{A}] = 0 \tag{38}$$

Firstly, we determined $\gamma^{\mathrm{nc}} = 10/11$ for the negative capacitor, so $\gamma^{\mathrm{nc}}/(1 - \gamma^{\mathrm{nc}}) = 10$. Fig. 9

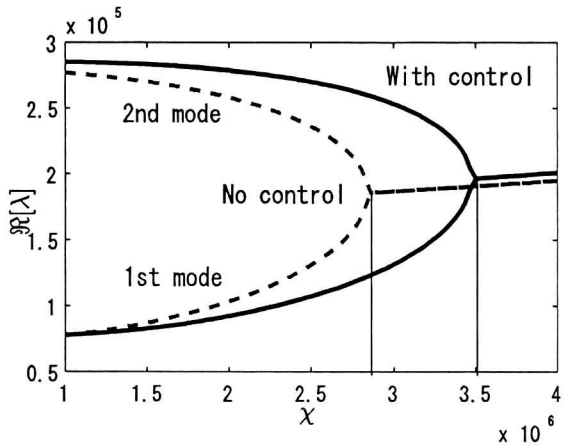

Fig. 9. Real part of eigenvalues as a function of dynamic pressure when $\gamma^{nc}/(1-\gamma^{nc}) = 10$ (control approach 2)

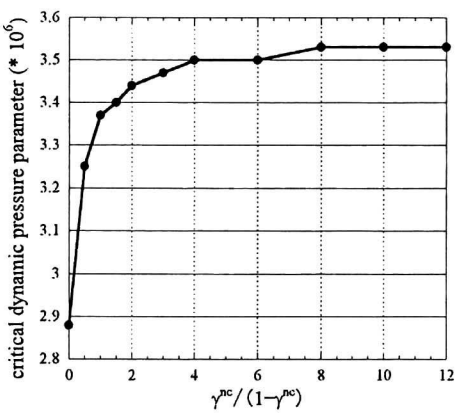

Fig. 10. Critical dynamic pressure parameter as a function of negative capacitance parameter (control approach 2)

plots the real part of eigenvalues as a function of dynamic pressure parameter, χ. The eigenvalues of the first and the second modes become close to each other as χ increased. When $\chi = 3.50\times10^6$, the two become one, i.e., $\Re[\lambda] = 1.97 \times 10^3$. With this critical value of χ, the wing experiences flutter phenomenon. It should be noted that the critical dynamic pressure increased by as much as 24 %.

Secondly, to investigate the relation between the critical dynamic pressure and the negative capacitance value, we varied $\gamma^{nc}/(1-\gamma^{nc})$ in the eigenvalue analysis. Fig. 10 plots the critical dynamic pressure parameter as a function of $\gamma^{nc}/(1-\gamma^{nc})$. The negative capacitance system with $\gamma^{nc}/(1-\gamma^{nc}) = 0$ means no control system. As seen from this figure, the critical dynamic pressure increases as $\gamma^{nc}/(1-\gamma^{nc})$ increases. However, the critical dynamic pressure parameter converges to 3.53×10^6 in this configuration.

Conclusions

We analyzed flutter suppression of a cantilevered plate wing, employing the finite element method and the quasi-steady aerodynamic theory. Two control approaches to flutter suppression using piezoelectric materials were presented; the energy-recycling semi-active approach and the negative capacitance approach. The use of smart circuits composed of piezoelectric materials and electric devices led to supersonic flutter suppression. The critical dynamic pressure increased by as much as 24 % for the wing with a negative capacitor and a piezoelectric patch attached to the wing surface. More experimental validation is essential for assessing flutter suppression performances, and an experiment is currently being prepared.

We evaluated flutter suppression approaches using piezoelectric materials in supersonic flutter problems. However, our control approaches can, in principle, be applied to other flutter problems, e.g., wing flutter problems in other speed ranges, or panel flutter problems.

References

[1] Dowell, E. H., "Nonlinear Oscillations of a Fluttering Plate," *AIAA Journal*, Vol. 4, No. 7, 1966, pp. 1267-1275.

[2] Matsuzaki, Y., and Ando, Y., "Estimation of Flutter Boundary from Random Responses Due to Turbulence at Subcritical Speeds," *Journal of Aircraft*, Vol. 18, No. 10, 1981, pp. 862-868.

[3] Lin, K. J., Lu, P. J., and Tarn, P. J., "Flutter Analysis of Cantilever Composite Plates in Subsonic Flow," *AIAA Journal*, Vol. 27, 1989, pp. 1102-1109.

[4] Lottati, I., "The Role of Structural and Aerodynamic Damping on the Aeroelastic Behavior of Wings," *Journal of Aircraft*, Vol. 23, 1986, pp. 606-608.

[5] Bae, J. S., Kim, J. Y., Lee, I., Matsuzaki, Y., and Inman, D. J., "Extension of Flutter Prediction Parameter for Multi-Mode Flutter System, *Journal of Aircraft*, Vol. 42, No. 1, 2005, pp. 285-288.

[6] Oh, I. K., Lee, I., and Lee, D. M., "Nonlinear Transient Response of Fluttering Stiffened Composite Plates Subject to Thermal Load," *Journal of Sound and Vibration*, Vol. 245, No. 4, 2002, pp. 715-736.

[7] Kameyama, M., and Fukunaga H., "Optimum Design of Composite Plate Wings for Aeroelastic Characteristics Using Lamination Parameters," *Computers and Structures*, (to be appeared).

[8] Odaka, Y., and Furuya, H., "Robust Structural Optimization of Plate Wing Corresponding to Bifurcation in Higher Mode Flutter," *Structural and Multidisciplinary Optimization*, Vol. 30, 2005, pp. 437-446.

[9] Zhou, R. C., Lai, Z., Xue, D. Y., Huang, J.-K., and Mei, C., "Suppression of Nonlinear Panel Flutter with Piezoelectric Actuators Using Finite Element Method," *AIAA Journal*, Vol. 33, No. 6, 1995, pp. 1098-1105.

[10] Moon, S. H., and Hwang, J. S., "Panel Flutter Suppression with an Optimal Controller Based on the Nonlinear Model Using Piezoelectric Materials," *Composite Structures*, Vol. 68, 2005, pp. 371-379.

[11] Han, J.-H., Tani, J., and Qiu, J., "Active Flutter Suppression of a Lifting Surface Using Piezoelectric Actuation and Modern Control Theory," *Journal of Sound and Vibration*, Vol. 291, 2006, pp. 706-722.

[12] Raja, S., Pashilkar, A. A., Sreedeep, R., and Kamesh, J. V., "Flutter Control of a Composite Plate

with Piezoelectric Multilayered Actuators," *Aerospace Science and Technology*, Vol. 10, 2006, pp. 435-441.

[13] Hagood, N. W., and von Flotow, A., "Damping of Structural Vibrations with Piezoelectric Patches and Passive Electrical Networks," *Journal of Sound and Vibration*, Vol. 146, No. 2, 1991, pp. 243-268.

[14] Wu, S., "Piezoelectric Shunts with a Parallel R-L Circuit for Structural Damping and Vibration Control," *Proc. SPIE Smart Structures and Materials Conference: Passive Damping and Isolation, San Diego*, CA, Vol. 2720, 1996, pp. 259-269.

[15] Moon, S. H., and Kim, S. J., "Active and Passive Suppressions of Nonlinear Panel Flutter Using Finite Element Method," *AIAA Journal*, Vol. 39, No. 11, 2001, pp. 2042-2050.

[16] Agneni, A., Mastroddi, F., and Polli, G. M., "Shunted Piezoelectric Patches in Elastic and Aeroelastic Vibrations," *Computers and Structures*, Vol. 81, 2003, pp. 91-105.

[17] Clark, W. W., "Vibration Control with State-Switched Piezoelectric Materials," *Journal of Intelligent Material Systems and Structures*, Vol. 11, No. 4, 2000, pp. 263-271.

[18] Richard, C., Guyomar, D., Audigier, D., and Ching, G., "Semi-Passive Damping Using Continuous Switching of a Piezoelectric Device," *Proc. SPIE Smart Structures and Materials Conference: Damping and Isolation, San Diego*, CA, Vol. 3672, 1999, pp. 104-111.

[19] Onoda, J., Makihara, K., and Minesugi, K., "Energy-Recycling Semi-Active Method for Vibration Suppression with Piezoelectric Transducers," *AIAA Journal*, Vol. 41, No. 4, 2003, pp. 711-719.

[20] Makihara, K., Onoda, J., and Minesugi, K., "Comprehensive Assessment of Semi-Active Vibration Suppression Including Energy Analysis," *ASME, Journal of Vibration and Acoustics*, (to be appeared).

[21] Corr, L. R., and Clark, W. W., "A Novel Semi-Active Multi-Modal Vibration Control Law for a Piezoceramic Actuator," *ASME, Journal of Vibration and Acoustics*, Vol. 125, No. 2, 2003, pp. 214-222.

[22] Makihara, K., Onoda, J., and Minesugi, K., "Novel Approach to Self-Sensing Actuation for Semi-Active Vibration Suppression," *AIAA Journal*, Vol. 44, No. 7, 2006, pp. 1445-1453.

[23] Badel, A., Guyomar, D., Lefeuvre, E., and Richard, C., "Efficiency Enhancement of a Piezoelectric Energy Harvesting Device in Pulsed Operation by Synchronous Charge Inversion," *Journal of Intelligent Material Systems and Structures*, Vol. 16, No. 10, 2005, pp. 889-901.

[24] Makihara, K., Onoda, J., and Miyakawa, T., "Low Energy Dissipation Electric Circuit for Energy-Harvesting Method," *Smart Materials and Structures*, Vol. 15, 2006, pp. 1493-1498.

[25] Makihara, K., Onoda, J., and Minesugi, K., "New Approach to Semi-Active Vibration Isolation to Improve the Pointing Performance of Observation Satellites," *Smart Materials and Structures*, Vol. 15, 2006, pp. 342-350.

[26] Ashley, H., and Zartarian, G., "Piston Theory - A New Aerodynamic Tool for the Aeroelastician," *Journal of the Aeronautical Sciences*, Vol. 23, 1956, pp. 1109-1118.

[27] Jaffe, B., Cook, W. R. Jr., and Jaffe, H., "Piezoelectric Ceramics," *Academic Press*, London, 1971.

[28] Zienkiewicz, O. C., and Taylor, R. L., "The Finite Element Method," *McGraw-Hill Book Company*, Berkshire, England, 1985.

[29] Tang, J., and Wang, K. W., "Active-Passive Hybrid Piezoelectric Networks for Vibration Control: Comparisons and Improvement," *Smart Materials and Structures*, Vol. 10, 2001, pp. 794-806.

[30] Lin, Q., and Rixen, D. J., "Self-Switching and Resistive Circuits for a Piezo Patch in Vibration Suppression," *Smart Materials and Structures*, Vol. 15, 2006, pp. 518-528.

[31] Neubauer, M., Oleskiewicz, R., Popp, K., and Krzyzynski, T., "Optimization of Damping and Absorbing Performance of Shunted Piezo Elements Utilizing Negative Capacitance," *Journal of Sound and Vibration*, Vol. 298, 2006, pp. 84-107.